On the Mechanics of Natural Compliance in Frictional Contacts and its Effect on Grasp Stiffness and Stability

Amir Shapiro* Dept. of ME, Ben Gurion University, ashapiro@bgu.ac.il

Elon Rimon Dept. of ME, Technion, rimon@technion.ac.il

Abstract *This paper considers the effect of natural material compliance on the stiffness and stability of frictional multi-contact grasps and fixtures. The contact preload profile is a key parameter in the nonlinear compliance laws governing such contacts. The paper introduces the Hertz-Walton contact compliance model which is valid for linear contact loading profiles. The model is specified in a lumped parameter form suitable for on-line grasping applications, and is entirely determined by the contact friction and by the material and geometric properties of the contacting bodies. The model predicts an asymmetric stiffening of the tangential reaction force as the normal load at the contact increases. As a result, the composite stiffness matrix of multi-contact grasps governed by natural compliance effects is asymmetric, indicating that these contact arrangements are not governed by any potential energy function. The implication of asymmetric grasp stiffness matrices on grasp stability is investigated. Based on the compliant grasp dynamics, the paper derives rules indicating which contact point locations and what preload profiles guarantee grasp and fixture stability. The paper also describes preliminary experiments supporting the contact model predictions.*

1 Introduction

This paper considers the effect of natural material compliance in frictional multi-contact arrangements. Natural friction-compliance effects play a key role in several grasping applications. For instance, biomimetic multi-finger hands are currently being developed for handling delicate objects such as fruits and vegetables [29, 36]. Such hands are typically designed with soft fingertips [14, 28], and the determination of grasp stability during ob-

*Corresponding author: Dept. of ME, Ben Gurion University, Beer-Sheva, Israel.

ject handling is a key component of these systems [35, 24, 43]. Natural contact compliance also plays an important role in quasistatic locomotion synthesis. When a multi-limbed or snake-like robot moves quasistatically by embracing against the environment, natural force-displacement laws at the contacts influence the mechanism's overall stability [31, 33]. A similar observation holds for whole arm manipulation, where a robot arm is allowed to establish mid-link contacts with the manipulated object [10, 27]. Due to the passive nature of the mid-link contacts, the stability of whole-arm grasps requires a consideration of the natural friction-compliance laws at the contacts [41]. Industrial fixturing may also benefit from friction-compliance stability models. Current fixturing practice immobilizes a given workpiece using redundant form closure grasps (e.g. [3, 4, 15, 16]). These costly arrangements rely on frictionless rigid-body constraints imposed by the fixturing elements. Sound understanding how natural compliance affects the stiffness and stability of frictional multi-contact arrangements will allow synthesis of more economic fixtures that rely on a smaller number of contacts [37].

The natural stiffness and stability of multi-contact arrangements is determined by nonlinear compliance laws. When these laws model frictional compliant contacts, these laws require explicit consideration of the contact loading profiles. The Hertz-Walton model provides an analytic compliance law under the assumption of *linear* contact loading profiles. Based on this model, the current paper analyzes the stiffness and stability of multi-contact grasps and fixtures and derives rules indicating which contact point locations and what preload profiles guarantee stable grasps. The relevant literature can be divided into compliance models proposed in the solid mechanics literature, and natural compliance grasp analysis and synthesis tools developed in the robotics literature.

In the solid mechanics literature, the modeling of the *normal* force due to natural compliance effects is based on the classical model of Hertz [12]. The main focused effort on modeling the natural *tangential* compliance at a non-slipping frictional contact is by Mindlin and Deresiewicz [22, 23]. They investigated the case where a contact is initially loaded along the normal direction in accordance with the Hertz compliance model. Then they analyzed the tangential traction field generated by applying pure tangential loads while the normal load remains constant. Their investigation revealed highly nonlinear and complex phenomena such as micro-slip and hysteresis. Moreover, researchers in this field have come to realize that the tangential force-displacement law depends on the contact's loading profile [18][p. 221]. Motivated by granular material packing applications, Walton [38] derived an analytic tangential compliance model which is much more relevant for grasping and fixturing applications. This model was later refined by Elata and Berryman [6]. Walton assumes that a contact is loaded along some *linear loading profile.* Under this assumption (and using a different analysis approach than Mindlin's), he derived an analytic model for the tangential compliance force at a frictional contact. The normal force component in Walton's

model satisfies the Hertz law, and the combined Hertz-Walton model will be the basis for the investigation conducted in this paper. The solid mechanics literature also offers numerical compliance models based on finite-element analysis (e.g. [7, 42]). However, an analytic lumped-parameter models provide the insight and computational simplicity required for automated grasp and fixture planning [19].

In the robotics literature, the stability of multi-contact grasps and fixtures is generally determined by their *stiffness matrix*, giving the linearized relation between small movements of the grasped object and the net reaction wrench (force and torque) generated by the contacts. Early papers attempted to model natural compliance effects by postulating linear springs that act in tandem with a rigid-body Coulomb friction law [1, 9]. A positive definite Hessian matrix of the springs' elastic potential energy ensures stability of such grasps [26, 40]. However, the linear spring approach is not supported by the solid mechanics literature. In particular, without knowledge of an underlying nonlinear contact model there is no way to predict the linear spring coefficients. Moreover, it is intuitively clear (and rigorously justified below) that the contacts experience tangential stiffening as the bodies are pressed harder together. Subsequent papers focused on the inclusion of the Hertz normal compliance model into the analysis and synthesis of *frictionless* grasps and fixtures [17, 20, 21, 43]. The first systematic efforts at incorporating *frictional* compliance effects were made by Francois, Ikeuchi, and Hebert [8], and by Sinha and Abel [34, 19, 39]. However, they proposed discretized friction-compliance contact models akin to the finite-element approach. This paper considers analytic compliance models that allow closed form analysis and synthesis of stable grasps.

Xiong et al. have recently combined Sinha and Abel's contact model with the Hertz normal compliance model [41]. They obtained a nonlinear compliance model which predicts the normal and tangential contact reaction forces, and applied this model to the prediction of stability and force closure in whole-arm grasps. Our paper complements their work in three fundamental ways. First, their contact model requires that the contacts be preloaded only along the contact normals. The Hertz-Walton model allows any linear loading of the contacts. Second, they judge the stability of a candidate grasp by constructing a potential energy function and computing its Hessian matrix. While a potential-function approach may be justified under normal loading profiles, this paper establishes that under general linear loading profiles the resulting grasp is not governed by any potential energy function. Third, the current paper emphasizes the role of the contact loading profile in ensuring grasp stability, a topic which has not yet been discussed in the robotics literature.

The paper is structured as follows. Section 2 describes the Hertz-Walton compliance model associated with linear contact loading profiles. Section 3 focuses on the stiffness matrices of the individual contacts, which are shown to be *asymmetric* under the Hertz-Walton model. Section 3 derives the composite grasp stiffness matrix associated with the

Hertz-Walton model. The grasp stiffness matrix is *asymmetric,* thus indicating that the dynamics of frictional multi-contact grasps and fixtures is *not* governed by any potential energy function. To establish the stability of such grasps and fixtures, Section 3 characterizes which linear loadings profiles guarantee stable response at the individual contacts. Based on this characterization, Section 4 analyzes the composite grasp dynamics and derives a local stability criterion that can be interpreted as a rule for selecting contact point locations which guarantee grasp stability. Section **??** describes experiments which verify the Hertz-Walton model using compliant fingertip material. The concluding section discusses `extension to 3D` and on-going experimental validation of the model predictions.

2 Friction-Compliance Models

This section describes the Hertz and Walton compliance models in a configuration-space setting. Assume that a 3D object $\mathcal{B}$ is held stationary by 3D bodies $\mathcal{A}_1, \ldots, \mathcal{A}_k$ representing fingertips or fixels. The usual assumption made in the solid mechanics literature is that the contacting bodies are *quasi-rigid*, meaning that their deformations due to natural compliance effects are localized to the vicinity of the contacts [18]. This assumption is generally valid for all bodies which are not made of exceptionally soft material and do not contain slender substructures [43]. The quasi-rigidity assumption allows us to describe the overall motion of $\mathcal{B}$ relative to the stationary bodies $\mathcal{A}_1, ..., \mathcal{A}_k$ using rigid body kinematics. Since the grasping bodies are essentially stationary, one can focus on $\mathcal{B}$'s configuration space, or *c-space.*

This paper considers the nonlinear compliance models in the context of planar configuration spaces. We assume that the bodies lie on a frictionless supporting plane, such that the bodies interact via frictional forces parallel to the supporting plane. The planar configuration of $\mathcal{B}$ is parametrized by $q = (d, \theta) \in \mathbb{R}^2 \times \mathbb{R}$, where d and θ are $\mathcal{B}$'s position and orientation relative to a fixed reference frame. The velocities of $\mathcal{B}$ are denoted $\dot{q} = (v, \omega) \in \mathbb{R}^2 \times \mathbb{R}$, where v and ω are $\mathcal{B}$'s linear and angular velocities. The wrenches acting on $\mathcal{B}$ are denoted $\boldsymbol{w} = (f, \tau) \in \mathbb{R}^2 \times \mathbb{R}$, where f and τ are the force and torque acting on $\mathcal{B}$. Note that $\boldsymbol{w}$ acts as a covector on $\dot{q}$, with $\boldsymbol{w} \cdot \dot{q}$ corresponding to the physical power transmitted to $\mathcal{B}$ during its instantaneous motion along $\dot{q}$.

2.1 Normal Compliance Models

Let us first describe a generic normal compliance modeling approach which ignores the details of compliant surface deformation and models the resultant contact force as a function of $\mathcal{B}$'s configuration [20]. Consider a single contact between $\mathcal{B}$ and $\mathcal{A}_i$. In the absence of deformation, the two bodies contact at a single point. When pushed together, the two

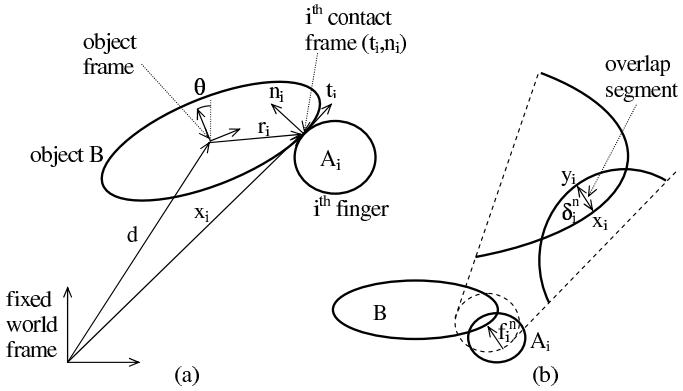

Figure 1: (a) The parametrization of $\mathcal{B}$'s c-space by (d, θ). (b) The overlap segment between $\mathcal{B}$ and $\mathcal{A}_i$ and the net normal force acting along this segment.

contacting surfaces deform. One can conceptually think of the two rigid bodies as interpenetrating, or overlapping with their undeformed shapes, as illustrated in Figure 1(b). When $\mathcal{B}$ is located at a configuration q, the *overlap*[1] between $\mathcal{B}$ and $\mathcal{A}_i$, denoted $\delta_i^n(q)$, is the minimum amount of translation of $\mathcal{B}$ that would separate it from $\mathcal{A}_i$. The *overlap segment* is the unique segment whose endpoints lie on the surfaces of $\mathcal{B}$ and $\mathcal{A}_i$, such that the length of the segment is δ_i^n and its orientation gives the direction of separating translation. For sufficiently small δ_i^n, the overlap segment is collinear with the normals to the surfaces of $\mathcal{B}$ and $\mathcal{A}_i$. In this lumped parameter form of modeling, the net normal force induced by the local deformation is assumed to act at $\mathcal{B}$'s endpoint of the overlap segment, x_i, along the inward pointing direction of the overlap segment, n_i (Figure 1). The normal component of the contact force, f_i^n, is assumed to depend on δ_i^n in terms of a function $g_i(\delta_i^n)$. This function is required to be differentiable, zero when δ_i^n is zero, and monotonically increasing when δ_i^n is positive. The normal component of the contact force, f_i^n, obeys a generic law of the form:

$$f_i^n = g_i(\delta_i^n) + \delta_i^n \cdot \varphi_i^n(\dot{\delta}_i^n)$$
$$\text{such that } g_i'(\delta_i^n) > 0 \text{ when } \delta_i^n > 0.$$

It is important to note that a wide variety of contact models can be represented under this generic law. The simplest contact model assumes that g_i is a linear function of the overlap: $g_i(\delta_i^n) = \kappa_i \delta_i^n$, where the coefficient κ_i represents the combined stiffness of $\mathcal{B}$ and $\mathcal{A}_i$ at the contact [17]. The function φ_i^n represents damping due to viscoelastic effects. It is required to be differentiable, zero when $\dot{\delta}_i^n$ is zero, and monotonically increasing in $\dot{\delta}_i^n$. Note that φ_i^n is positive when the damping force acts along $\mathcal{B}$'s inward contact normal. The damping force

[1]The notion of overlap used here is consistent with the concept of "relative approach" in contact mechanics [18].

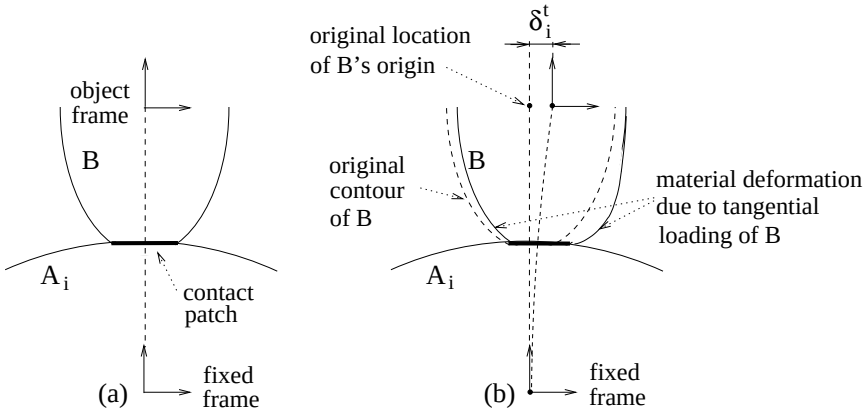

Figure 2: (a) An initial contact area generated by normal loading of $\mathcal{B}$ against $\mathcal{A}_i$. (b) Tangential loading of $\mathcal{B}$ causes tangential displacement of $\mathcal{B}$ without any macro-slip.

thus resists $\mathcal{B}$'s penetration into $\mathcal{A}_i$ when $\dot{\delta}_i^n > 0$, and resists $\mathcal{B}$'s motion away from $\mathcal{A}_i$ when $\dot{\delta}_i^n < 0$.

The Hertz normal compliance model [12]. The nonlinear Hertz model which has been verified experimentally [18], establishes that for two quasi-rigid bodies with spherical tips of radii r_1 and r_2:

$$g_i(\delta_i^n) = \frac{8G\sqrt{r}}{3(1-\nu)}(\delta_i^n)^{3/2}, \tag{1}$$

where $r = r_1 r_2/(r_1+r_2)$, G is the material's modulus of rigidity expressed in N/m^2, and ν is the material's Poisson ratio. The Poisson ratio is a unitless parameter satisfying $0 \leq \nu \leq 0.5$ for all practical materials [18]. The Hertzian law is sometimes expressed in terms of the material's modulus of elasticity, E, rather than G, where $E=2G(1+\nu)$.

2.2 Tangential Compliance Models

The process underlying tangential compliance at a frictional contact is as follows. When two quasi-rigid bodies are preloaded along the normal direction, they locally deform and establish a contact area centered at the original contact point (Figure 2(a)). The deformed bodies generate a normal force-field which is continuously distributed along the contact area (its integral over the contact area gives the net normal force f_i^n). When the two bodies are next loaded along a tangential direction, they locally deform in a way that generates a tangential force-field which is again continuously distributed along the contact area (Figure 2(b)). The usual assumption made in the solid mechanics literature is that *the normal and tangen-*

tial force fields interact at the individual points of the contact area according to Coulomb's law [23]. Under this assumption, elasticity theory as well as experiments indicate that the tangential force-field consists of two regimes. At points in an outer ring of the contact area the tangential forces exceed the friction cone constraint, causing micro-slip at these points. At points along the complementary inner disc of the contact area the tangential forces lie within the friction cone, and at these points no micro-slip takes place. As the magnitude of the tangential loading increases the area of the stationary inner disc shrinks. Finally, when the net tangential force reaches μf_i^n (μ being the coefficient of friction), the inner disc shrinks to a point and the two bodies experience macro-slip at the contact.

Based on this insight, we formulate a generic tangential compliance law, assuming that the contacting bodies deform but do not slip. This law covers most of the tangential compliance models proposed in the literature [6, 23, 38], and is therefore quite general. Recall that x_i is $\mathcal{B}$'s endpoint of the overlap segment. Let r_i denote the same point expressed in $\mathcal{B}$'s body frame (Figure 1(a)). Then x_i is related to r_i by the rigid-body transformation: $x_i = X(r_i, q) = R(\theta)r_i + d$, where $R(\theta)$ is $\mathcal{B}$'s orientation matrix. Let $X_{r_i}(q)$ denote the transformation $X(r_i, q)$ such that r_i is held fixed. When $\mathcal{B}$ moves along a c-space trajectory $q(t)$, the velocity of X_{r_i} is given by $\frac{d}{dt}X_{r_i}(q(t)) = G_i\dot{q}(t)$, where $G_i = DX_{r_i}$ is the 2×3 Jacobian matrix of X_{r_i}. Let $\delta_i^t(q(t))$ denote the tangential displacement of $\mathcal{B}$ relative to the i^{th} contact due to $\mathcal{B}$'s motion along $q(t)$ (Figure 2(b)). Let t_i denote the unit tangent to $\mathcal{B}$'s boundary at x_i. The derivative of δ_i^t along $q(t)$ is given by the projection of $\dot{X}_{r_i}$ along t_i:

$$\frac{d}{dt}\delta_i^t(q(t)) = t_i \cdot \dot{X}_{r_i} = t_i \cdot G_i\dot{q}(t). \tag{2}$$

In contrast with $\delta_i^n(q)$, the tangential displacement is *not* a direct function of q, but requires integration of (2) over the entire loading trajectory [18][p. 221]. The tangential component of the contact force, f_i^t, obeys a generic law of the form:

$$\begin{aligned} f_i^t = &-h_i(\delta_i^t, \delta_i^n) - \delta_i^n \cdot \varphi_i^t(\dot{\delta}_i^t) \\ &\text{as long as } f_i^n > 0 \text{ and } |f_i^t| < \mu f_i^n, \end{aligned}$$

where μ is the coefficient of friction. The function representing the elastic component of the tangential force, $h_i(\delta_i^t, \delta_i^n)$, depends both on the tangential and normal displacements. This function is required to be differentiable, zero when δ_i^n is zero, and for any fixed positive δ_i^n monotonically increasing in δ_i^t. The negative sign preceding h_i implies that the tangential force *opposes* the direction of tangential displacement. The function φ_i^t represents damping due to micro-slip. It is required to be differentiable, zero when $\dot{\delta}_i^t$ is zero, and monotonically increasing in $\dot{\delta}_i^t$. The negative sign preceding φ_i^t indicates that its force resists the instantaneous change in δ_i^t.

Walton's tangential compliance model [38]. Walton assumes that a contact is loaded along a linear loading profile satisfying $\delta_i^t = c_i \delta_i^n$, such that c_i is constant throughout the loading process. When two quasi-rigid bodies with spherical tips of radii r_1 and r_2 are preloaded with a linear loading profile, the function h_i is given by

$$\begin{aligned} h_i(\delta_i^t, \delta_i^n) &= \tfrac{16G\sqrt{r}}{3(2-\nu)} \sqrt{\delta_i^n}\, \delta_i^t \\ &\qquad \text{as long as } \delta_i^n > 0 \text{ and } |c_i| < \mu \tfrac{(2-\nu)}{2(1-\nu)}, \end{aligned} \tag{3}$$

where G and ν are specified above, $r = r_1 r_2/(r_1+r_2)$, and μ is the friction coefficient at the contact. The condition $|c_i| \leq \mu \frac{(2-\nu)}{2(1-\nu)}$ results from substituting formulas (1) and (3) for f_i^n and f_i^t in the friction cone constraint $|f_i^t| < \mu f_i^n$. Walton's formula is extremely relevant for grasping and fixturing applications, since one can readily implement a linear preloading of the contacts. Note that (3) indicates a nonlinear tangential stiffening at the contact for larger normal penetrations. Walton's formula agrees up to constants with the tangential compliance model obtained by Mindlin and Deresiewicz [22, 23]. However, the Mindlin and Deresiewicz model assumes pure normal loading followed by pure tangential loading, while the Walton model allows any linear loading profile.

3 The Individual Contact Stiffness Matrices

When a quasi-rigid object $\mathcal{B}$ is held in a compliant equilibrium grasp, the grasp's stability is determined by the net wrench induced on $\mathcal{B}$ by the contacts in response to small displacements of $\mathcal{B}$. This section characterizes the wrench induced on $\mathcal{B}$ by the individual contacts under the Hertz-Walton compliance model. Let q_0 denote the object's equilibrium grasp configuration, which is assumed to be preloaded in accordance with the Hertz-Walton model. Denote by f_i the i^{th} contact force acting on $\mathcal{B}$ at x_i, described in a fixed reference frame. Denote by t_i and n_i the unit tangent and inward unit normal to $\mathcal{B}$ at x_i, and by $R_i(q_0) = [t_i\, n_i]$ the 2×2 orientation matrix of the i^{th} contact frame at q_0. The force f_i is given by

$$f_i = R_i(q_0) \begin{pmatrix} f_i^t \\ f_i^n \end{pmatrix},$$

where (f_i^t, f_i^n) are specified in terms of (δ_i^t, δ_i^n) by the Hertz-Walton model. The i^{th} *contact stiffness matrix*, $K_i(q_0)$, is the 2×2 matrix representing the linearized force-displacement relationship at the i^{th} contact:

$$\begin{pmatrix} \Delta f_i^t \\ \Delta f_i^n \end{pmatrix} = K_i(q_0) \begin{pmatrix} \Delta \delta_i^t \\ \Delta \delta_i^n \end{pmatrix}, \tag{4}$$

where $K_i(q_0)$ is specified below. The matrix $K_i(q_0)$ induces a wrench-displacement relationship in $\mathcal{B}$'s c-space as follows. Let $\Delta q = q - q_0$ denote a small c-space displacement of $\mathcal{B}$ about q_0. Let $\Delta \boldsymbol{w}_i$ be the wrench generated by the i^{th} contact on $\mathcal{B}$ due to the displacement Δq. Using the notation $\boldsymbol{\delta}_i(q) = (\delta_i^t(q), \delta_i^n(q))$, the pair $(\Delta f_i^t, \Delta f_i^n)$ is related to Δq by

$$\begin{pmatrix} \Delta f_i^t \\ \Delta f_i^n \end{pmatrix} = K_i(q_0) D\boldsymbol{\delta}_i(q_0) \Delta q, \tag{5}$$

where $D\boldsymbol{\delta}_i$ is the 2×3 Jacobian of $\boldsymbol{\delta}_i(q)$. The wrench induced by $(\Delta f_i^t, \Delta f_i^n)$ on $\mathcal{B}$ is given by $\Delta \boldsymbol{w}_i = G_i^T R_i \begin{pmatrix} \Delta f_i^t \\ \Delta f_i^n \end{pmatrix}$, where $G_i = DX_{r_i}$ is the 2×3 Jacobian of X_{r_i}. Multiplying both sides of (5) by $G_i^T R_i$ gives the c-space relation:

$$\Delta \boldsymbol{w}_i = \left[G_i^T(q_0) R_i(q_0) K_i(q_0) D\boldsymbol{\delta}_i(q_0) \right] \Delta q = \tilde{K}_i(q_0) \Delta q.$$

The 3×3 matrix $\tilde{K}_i(q_0)$ is the linearized wrench-displacement relationship induced on $\mathcal{B}$ by the i^{th} contact.

We now derive formulas for $K_i(q_0)$ and $\tilde{K}_i(q_0)$ based on the Hertz-Walton model. Walton's law assumes a linear loading profile. It is therefore valid only for small changes $(\Delta\delta_i^t, \Delta\delta_i^n)$ aligned with the nominal loading profile. On the other hand, $K_i(q_0)$ gives the contact reaction force in response to arbitrary small displacements $(\Delta\delta_i^t, \Delta\delta_i^n)$. To obtain a formula for $K_i(q_0)$, we introduce the practical assumption that *closely matching loading profiles generate closely matching tangential traction fields.* Under this assumption the tangential traction field resulting from a linear loading followed by arbitrary small displacements can be obtained from the Hertz-Walton model. The formulas for $K_i(q_0)$ and $\tilde{K}_i(q_0)$ are as follows.

Lemma 3.1. *Let two quasi-rigid bodies with spherical tips of radii r_1 and r_2 be preloaded along a linear path $\delta_i^t(q) = c_i \delta_i^n(q)$ such that $|c_i| < \mu \frac{(2-\nu)}{2(1-\nu)}$. The i^{th} contact stiffness matrix under the Hertz-Walton law is the 2×2 matrix:*

$$K_i(q_0) = 4G\sqrt{r}\sqrt{\delta_i^n(q_0)} \begin{bmatrix} -\frac{4}{3(2-\nu)} & -\frac{2c_i}{3(2-\nu)} \\ 0 & \frac{1}{1-\nu} \end{bmatrix}, \tag{6}$$

where $\delta_i^n(q_0)$ is the normal penetration, $r = r_1 r_2/(r_1 + r_2)$, and G and ν are the material's shear modulus and Poisson ratio. The c-space stiffness matrix induced by $K_i(q_0)$ is the 3×3 matrix:

$$\tilde{K}_i(q_0) = -4G\sqrt{r}\sqrt{\delta_i^n(q_0)} G_i^T(q_0) R_i(q_0) \begin{bmatrix} \frac{4}{3(2-\nu)} & -\frac{2c_i}{3(2-\nu)} \\ 0 & \frac{1}{1-\nu} \end{bmatrix} R_i^T(q_0) G_i(q_0), \tag{7}$$

where $R_i(q_0) = [t_i \; n_i]$ and $G_i = DX_{r_i}$.

Note that $K_i(q_0)$ and consequently $\tilde{K}_i(q_0)$ are *asymmetric* matrices. The implication of this asymmetry on the stiffness and stability of multi-contact grasps is investigated in the next section.

Proof: The formula for $K_i(q_0)$ is obtained by taking the derivative of (f_i^t, f_i^n) given in (1) and (3) with respect to (δ_i^t, δ_i^n), then substituting the loading path relation $\delta_i^t(q_0) = c_i\delta_i^n(q_0)$. Next consider the 3×3 matrix $\tilde{K}_i(q_0) = G_i^T(q_0)R_i(q_0)K_i(q_0)D\boldsymbol{\delta}_i(q_0)$. Since $\boldsymbol{\delta}_i = (\delta_i^t, \delta_i^n)$, the rows of the 2×3 Jacobian $D\boldsymbol{\delta}_i(q_0)$ are the differentials $D\delta_i^t(q_0)$ and $D\delta_i^n(q_0)$. Since $\frac{d}{dt}\delta_i^t(q(t)) = t_i\cdot G_i(q(t))\dot{q}$ according to (2), $D\delta_i^t = t_i^T G_i$. Similarly, it can be verified that $\frac{d}{dt}\delta_i^n(q(t)) = -n_i\cdot G_i(q(t))\dot{q}$ [30], and consequently $D\delta_i^n = -n_i^T G_i$.[2] The formula for $D\boldsymbol{\delta}_i(q_0)$ is thus $D\boldsymbol{\delta}_i(q_0) = \left[\begin{smallmatrix} t_i^T \\ -n_i^T \end{smallmatrix}\right] G_i(q_0)$. Substituting for $K_i(q_0)$ and $D\boldsymbol{\delta}_i(q_0)$ in the product $K_i(q_0)D\boldsymbol{\delta}_i(q_0)$ gives

$$\begin{aligned} K_i(q_0)D\boldsymbol{\delta}_i(q_0) &= \begin{bmatrix} -\frac{4}{3(2-\nu)} & -\frac{2c_i}{3(2-\nu)} \\ 0 & \frac{1}{1-\nu} \end{bmatrix} \begin{bmatrix} t_i^T \\ -n_i^T \end{bmatrix} G_i(q_0) \\ &= -\begin{bmatrix} \frac{4}{3(2-\nu)} & -\frac{2c_i}{3(2-\nu)} \\ 0 & \frac{1}{1-\nu} \end{bmatrix} \begin{bmatrix} t_i^T \\ n_i^T \end{bmatrix} G_i(q_0) \\ &= -\begin{bmatrix} \frac{4}{3(2-\nu)} & -\frac{2c_i}{3(2-\nu)} \\ 0 & \frac{1}{1-\nu} \end{bmatrix} R_i^T(q_0)G_i(q_0), \end{aligned}$$

where we omitted the scalars preceding $K_i(q_0)$ and substituted $R_i^T = \left[\begin{smallmatrix} t_i^T \\ n_i^T \end{smallmatrix}\right]$. Pre-multiplying the latter expression by $G_i^T(q_0)R_i(q_0)$ gives the formula for $\tilde{K}_i(q_0)$. □

In preparation for the grasp stability analysis conducted in the next section, we need to establish when the symmetric part of $\tilde{K}_i(q_0)$, $(\tilde{K}_i(q_0))_s = \frac{1}{2}\big(\tilde{K}_i(q_0) + \tilde{K}_i^T(q_0)\big)$, is negative semi-definite. A key result is that the negative semi-definiteness of $(\tilde{K}_i(q_0))_s$ depends solely on the slope of the linear loading profile.

Proposition 3.2. *Let the i^{th} contact be loaded along a linear loading profile with slope c_i. If the loading profile satisfies the inequality*

$$|c_i| < 2\sqrt{\frac{3(2-\nu)}{(1-\nu)}}, \tag{8}$$

the symmetrized stiffness matrix induced by the i^{th} contact, $\big(\tilde{K}_i(q_0)\big)_s$, is negative semi-definite.

[2] Since n_i points into $\mathcal{B}$ and $\dot{x}_i = G_i\dot{q}$, $\frac{d}{dt}\delta_i^n(q(t)) = (-n_i)\cdot\dot{x}_i > 0$ means that $\mathcal{B}$ penetrates deeper into $\mathcal{A}_i$, while the converse holds when $\frac{d}{dt}\delta_i^n(q(t)) < 0$.

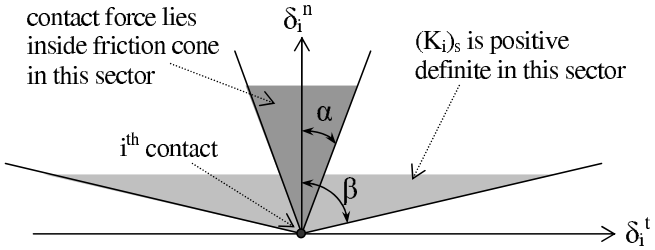

Figure 3: The sectors in the (δ_i^t, δ_i^n)-plane associated with a positive semi-definite $(\tilde{K}_i)_s$ and the friction cone constraint. Typically $\alpha < 56.3°$ while $\beta < 80.5°$.

Proof: Denote by A_i the 2×2 matrix at the core of $\tilde{K}_i(q_0)$ in (7):

$$A_i = \begin{bmatrix} \frac{4}{3(2-\nu)} & -\frac{2c_i}{3(2-\nu)} \\ 0 & \frac{1}{1-\nu} \end{bmatrix}.$$

Then $(\tilde{K}_i)_s = -G_i^T R_i (A_i)_s R_i^T G_i$, where we omitted the positive scalars preceding $\tilde{K}_i$. The positive definiteness of $(A_i)_s$ implies the negative semi-definiteness of $(\tilde{K}_i)_s$. The 2×2 matrix $(A_i)_s$ is positive definite when its two eigenvalues, λ_1 and λ_2, are strictly positive. First consider the trace of $(A_i)_s$, $\mathsf{tr}(A_i)_s = \lambda_1 + \lambda_2$. Inspection of the diagonal elements in $(A_i)_s$ reveals that $\mathsf{tr}(A_i)_s > 0$ when $\nu < 1$. Since Poisson's ratio satisfies $0 \leq \nu \leq 0.5$ for all practical materials, $\mathsf{tr}(A_i)_s > 0$. Next consider the determinant of $(A_i)_s$, $\det(A_i)_s = \lambda_1 \lambda_2$. Since $\lambda_1 + \lambda_2 > 0$, a positive determinant would imply positive definiteness of $(A_i)_s$. The determinant of $(A_i)_s$ is:

$$\det(A_i)_s = \frac{4}{3(1-\nu)(2-\nu)} - \frac{c_i^2}{9(2-\nu)^2}.$$

The inequality $\det(A_i)_s > 0$ becomes $4/(1-\nu) > c_i^2/3(2-\nu)$. A square root of both sides gives the condition for the positive definiteness of $(A_i)_s$, which implies the negative semi-definiteness of $(\tilde{K}_i)_s$. □

Example: Figure 3 depicts the restriction imposed on the linear loading profile by (8). Since $\nu \leq 0.5$, the slope of the linear loading path must satisfy $|c_i| < 6.0$ for $(\tilde{K}_i)_s$ to be negative semi-definite. The corresponding slope angle, denoted β in Figure 3, must satisfy $|\beta| < 80.5°$. However, c_i must also satisfy the friction cone constraint $|c_i| < \mu(2-\nu)/2(1-\nu)$. For typical values of $\mu \leq 1$, the linear loading path's slope must satisfy the inequality $|c_i| < 1.5$. The corresponding slope angle, denoted α in Figure 3, must satisfy $|\alpha| < 56.3°$. It follows that the negative semi-definiteness of $(\tilde{K}_i)_s$ is typically *less restrictive* than the friction cone constraint. Since the linear loading path must always satisfy the friction cone constrain, the matrix $(\tilde{K}_i)_s$ is automatically negative semi-definite in typical linearly loaded grasps.

4 Grasp Stiffness and Stability Analysis

Based on the wrench-displacement relationship induced on $\mathcal{B}$ by the individual contacts, this section characterizes the stiffness and stability of frictional multi-contact grasps governed by the Hertz-Walton compliance model. Section 4.1 derives the linearized dynamics of $\mathcal{B}$ at a multi-contact grasp governed by the Hertz-Walton compliance model. The resulting grasp dynamics is governed by an asymmetric grasp stiffness matrix. Section 4.2 introduces a generic stability criterion for asymmetric linear systems [32]. Based on this criterion, we obtain the conditions under which the object is stably held by the compliant contacts.

4.1 Linearized Grasp Dynamics

Let a quasi-rigid object $\mathcal{B}$ be held in equilibrium grasp by quasi-rigid bodies $\mathcal{A}_1, \ldots, \mathcal{A}_k$. The bodies are assumed to lie on a frictionless plane such that the inter-body forces are parallel to this plane. The undeformed bodies are assumed to have spherical surfaces at the contacts, and the contacts are assumed to be preloaded along linear loading profiles in accordance with the Hertz-Walton model. The wrench induced on $\mathcal{B}$ by a contact force $f_i(q, \dot{q})$ acting at x_i is given by $G_i^T(q) f_i(q, \dot{q})$ where $G_i = DX_{r_i}(q)$ is the Jacobian of the transformation $x_i = X_{r_i}(q)$. The dynamics of $\mathcal{B}$ within the planar environment under the influence of k contact forces, without any other external influences, is given by

$$M(q)\ddot{q} + C(q, \dot{q}) = \sum_{i=1}^{k} G_i^T(q) f_i(q, \dot{q}), \tag{9}$$

where $M(q)$ is $\mathcal{B}$'s 3×3 inertia matrix, and $C(q, \dot{q})$ is the vector of centrifugal and Coriolis forces acting on $\mathcal{B}$. As before, q_0 denotes the object's equilibrium configuration. To determine the linearized dynamics of $\mathcal{B}$ at $(q, \dot{q}) = (q_0, 0)$, denote by $(p_1, p_2) = (q, \dot{q})$ the state variables of $\mathcal{B}$. Then (9) can be written as

$$\begin{array}{l} \dot{p}_1 = p_2 \\ \dot{p}_2 = M^{-1}(p_1)\big(\sum_{i=1}^{k} G_i^T(p_1) f_i(p_1, p_2) - C(p_1, p_2)\big). \end{array} \tag{10}$$

The following proposition describes the linearized dynamics of $\mathcal{B}$ at $(q_0, 0)$ (see Appendix A for a proof of the proposition).

Proposition 4.1. *Let a quasi-rigid $\mathcal{B}$ be held at an equilibrium grasp configuration, $q_0 = (d_0, \theta_0)$, by quasi-rigid bodies $\mathcal{A}_1, \ldots, \mathcal{A}_k$. Let $\Delta p_1 = q - q_0$ and $\Delta p_2 = \dot{q} - 0$. The linearized dynamics of $\mathcal{B}$ at $(q_0, 0)$ is given by*

$$\frac{d}{dt}\begin{pmatrix} \Delta p_1 \\ \Delta p_2 \end{pmatrix} = \begin{bmatrix} O_{3\times 3} & I_{3\times 3} \\ -M^{-1}(q_0)K_p(q_0, 0) & -M^{-1}(q_0)K_d(q_0, 0) \end{bmatrix} \begin{pmatrix} \Delta p_1 \\ \Delta p_2 \end{pmatrix}, \tag{11}$$

where K_p and K_d are the following grasp's stiffness and damping matrices. The grasp's stiffness matrix is the asymmetric 3×3 matrix:

$$K_p(q_0, 0) = -\sum_{i=1}^{k} \left\{ \tilde{K}_i(q_0) - \begin{bmatrix} O_{2\times 2} & 0 \\ 0^T & \boldsymbol{\rho}_i(\theta_0) \cdot f_i \end{bmatrix} + G_i^T(q_0) \begin{bmatrix} f_i^n & -f_i^t \\ f_i^t & f_i^n \end{bmatrix} Dn_i(q_0) \right\}, \quad (12)$$

where $\tilde{K}_i(q_0)$ is the c-space stiffness matrix induced by the i^{th} contact, $\boldsymbol{\rho}_i(\theta_0) = R(\theta_0) r_i$, f_i is the i^{th} contact force with components (f_i^t, f_i^n), and n_i is the i^{th} contact normal $(i = 1 \ldots k)$. The grasp's damping matrix is the symmetric 3×3 matrix:

$$K_d(q_0, 0) = \sum_{i=1}^{k} \delta_i^n(q_0) G_i^T(q_0) R_i(q_0) \begin{bmatrix} \frac{\partial \varphi_i^t}{\partial \dot{\delta}_i^t}(0) & 0 \\ 0 & \frac{\partial \varphi_i^n}{\partial \dot{\delta}_i^n}(0) \end{bmatrix} R_i^T(q_0) G_i(q_0), \quad (13)$$

where φ_i^t and φ_i^n are the tangential and normal damping functions at the i^{th} contact $(i = 1 \ldots k)$.

Let us discuss the meaning of the three terms appearing in the stiffness matrix K_p. The first term, $\sum_{i=1}^{k} \tilde{K}_i(q_0)$, gives the net wrench generated on $\mathcal{B}$ by the contacts under the Hertz-Walton compliance model. This term forms an asymmetric matrix, and the linearized grasp dynamics is consequently not governed by any potential energy function. The second term contains the sum $\sum_{i=1}^{k} \boldsymbol{\rho}_i(\theta_0) \cdot f_i$. This term represents the effect of the preload forces on the grasp stiffness matrix. When the preload level is too high this term can possibly destabilize the grasp, a phenomena known as "coin snapping" in the grasping literature [5, 20, 25]. The third term represents the overlap-segment change of direction due to small displacements of $\mathcal{B}$. This term depends on the curvature of the undeformed bodies at the contacts. As shown in Ref. [20], the 2×3 Jacobian $Dn_i(q_0)$ at the core of this term is given by

$$Dn_i(q_0) = \frac{1}{r_{\mathcal{A}_i} + r_{\mathcal{B}_i} + \delta_i^n(q_0)} [I_{3\times 3} - (\boldsymbol{\rho}_i(\theta_0) \cdot n_i) n_i n_i^T],$$

where $r_{\mathcal{A}_i}$ and $r_{\mathcal{B}_i}$ are the radii of curvature of $\mathcal{A}_i$ and $\mathcal{B}$ at the endpoints of the i^{th} overlap segment. As for the damping matrix, K_d, the normal penetration $\delta_i^n(q_0)$ is strictly positive at a preloaded contact. Since the damping functions φ_i^t and φ_i^n are monotonically increasing in their arguments, K_d is a symmetric positive definite matrix.

We will analyze the equilibrium grasps stability based on a generic stability criterion for asymmetric second-order linear systems [32]. To apply this criterion, we need to write the linearized grasp dynamics (11) in the standard form:

$$M(q_0)\Delta\ddot{q} + K_d(q_0, 0)\Delta\dot{q} + K_p(q_0, 0)\Delta q = \vec{0}, \quad (14)$$

where $\Delta q = q - q_0$ and $\Delta \dot{q} = \dot{q} - 0$. Note that $M(q_0)$ and $K_d(q_0, 0)$ are symmetric positive definite matrices while $K_p(q_0, 0)$ is an asymmetric matrix.

4.2 Stability of Second-Order Asymmetric Linear Systems

The local stability of a compliant equilibrium grasp can be determined from the linearization of the nonlinear grasp dynamics. When the contacts are governed by the Hertz-Walton compliance law, the linearized grasp dynamics forms an asymmetric second-order linear system (Proposition 4.1). The stability of such systems can be determined as follows. Given an $n \times n$ matrix A, $A_s = \frac{1}{2}(A + A^T)$ and $A_{as} = \frac{1}{2}(A - A^T)$ denote its symmetric and asymmetric parts, and $\|A\| = \max_{\|v\| \leq 1}\{\|Av\|\}$ for $v \in I\!R^n$ denote its norm. When A is additionally a symmetric matrix, its minimal eigenvalue is denoted $\lambda_{min}(A)$. The following theorem describes a generic criterion for the stability of asymmetric second-order linear systems.

Theorem 1 ([32]). *Consider the second-order linear system in the variable $p \in I\!R^n$,*

$$M\ddot{p} + K_d\dot{p} + K_p p = \vec{0}, \tag{15}$$

where $M \in I\!R^{n \times n}$ and $K_d \in I\!R^{n \times n}$ are symmetric positive definite matrices, while $K_p \in I\!R^{n \times n}$ is an asymmetric matrix such that $(K_p)_s$ is positive definite. Let $\alpha > 0$ be the minimal eigenvalue of $M^{-1/2}(K_p)_s M^{-1/2}$, let $\beta > 0$ be the minimal eigenvalue of $M^{-1/2} K_d M^{-1/2}$, and let $\gamma \geq 0$ be the matrix norm of $M^{-1/2}(K_p)_{as} M^{-1/2}$. If α, β, and γ satisfy the relation:

$$\gamma < \sqrt{\alpha}\beta$$

the system (15) is **globally asymptotically stable.**

The condition $\gamma < \sqrt{\alpha}\beta$ can be interpreted as follows. Consider the case where M is an identity matrix. Then $\alpha = \lambda_{min}\big((K_p)_s\big)$, $\beta = \lambda_{min}(K_d)$, and the condition $\gamma < \sqrt{\alpha}\beta$ becomes:

$$\|(K_p)_{as}\| < \lambda_{min}(K_d)\sqrt{\lambda_{min}\big((K_p)_s\big)}.$$

The stability condition essentially requires that the asymmetric part of K_p be sufficiently small relative to the symmetric part of K_p (modulated by the damping $\lambda_{min}(K_d)$). The following numerical example illustrates the applicability of the stability criterion.

Example: Consider the assymetric second-order linear system:

$$\begin{bmatrix} 10 & 0 \\ 0 & 11 \end{bmatrix} \ddot{p} + \begin{bmatrix} 4 & 1 \\ 1 & 5 \end{bmatrix} \dot{p} + \begin{bmatrix} 8 & s \\ -s & 9 \end{bmatrix} p = 0, \tag{16}$$

where s is a free parameter. The matrices M, K_d, and $(K_p)_s$ are all symmetric positive definite. Hence, when $s = 0$ the system is symmetric and asymptotically stable. Qualitatively, increasing the value of s increases the asymmetric part of the stiffness matrix. Calculation of α, β, and γ yields $\alpha = 4/5$, $\beta = 0.328$, and $\gamma = s/\sqrt{110}$. Therefore, the stability condition of Theorem 1 becomes the condition $|s| < 3.078$. For comparison we numerically calculated the eigenvalues of the 4×4 matrix $\begin{bmatrix} O & I \\ K_p & K_d \end{bmatrix}$. It turns out that for $0 \leq s < 3.920$ the system (16) is asymptotically stable (i.e. the eigenvalues of the 4×4 matrix lie in the left half of the complex plane). Thus, apart from being conservative, the stability condition (15) correctly predicts the system's global asymptotic stability.

The following key theorem applies the generic stability criterion, $\gamma < \sqrt{\alpha}\beta$, to the linearized grasp dynamics.

Theorem 2 (Compliant Grasp Stability)**.** *Let a quasi-rigid body $\mathcal{B}$ be grasped at an equilibrium q_0 by quasi-rigid bodies $\mathcal{A}_1, \ldots, \mathcal{A}_k$ satisfying the Hertz-Walton compliance law. Define the scalars α, β, and γ as*

$$\begin{aligned} \alpha &= \lambda_{min}\left(M^{-\frac{1}{2}}(q_0)(K_p(q_0,0))_s M^{-\frac{1}{2}}(q_0)\right) \\ \beta &= \lambda_{min}\left(M^{-\frac{1}{2}}(q_0) K_d(q_0,0) M^{-\frac{1}{2}}(q_0)\right) \\ \gamma &= \|M^{-\frac{1}{2}}(q_0)(K_p(q_0,0))_{as} M^{-\frac{1}{2}}(q_0)\|, \end{aligned}$$

where $M(q_0)$ is $\mathcal{B}$'s inertia matrix, $K_p(q_0,0)$ is the grasp's stiffness matrix, and $K_d(q_0,0)$ is the grasp's damping matrix.
If $\alpha > 0$, $\beta > 0$, and $\gamma < \sqrt{\alpha}\beta$, the zero-velocity state $(q_0, 0)$ of the nonlinear grasp dynamics (9) is **locally asymptotically stable.**

Proof: A nonlinear system $\dot{x} = F(x)$ has a *hyperbolic* equilibrium at x_0 when $F(x_0) = \vec{0}$ and the Jacobian $DF(x_0)$ has eigenvalues with non-zero real part [13]. When the system $\dot{x} = F(x)$ has a hyperbolic equilibrium at x_0, its local stability is fully determined by the linearized dynamics at x_0, a result known as the Hartman-Grobman lemma [11]. The linearized grasp dynamics at $(q_0, 0)$ has the form (see eq. (14)):

$$M(q_0)\Delta\ddot{q} + K_d(q_0)\Delta\dot{q} + K_p(q_0)\Delta q = 0. \tag{17}$$

Based on Theorem 1, the conditions $\alpha > 0$, $\beta > 0$, and $\gamma < \sqrt{\alpha}\beta$, ensure the global asymptotically stability of the linear system (17). Since an asymptotically stable equilibrium is necessarily hyperbolic, the nonlinear grasp dynamics is locally asymptotically stable. □

5 Synthesis of Compliantly Stable Grasps

This section discusses practical guidelines for synthesizing compliantly stable grasps and fixtures based on the stability criterion of Theorem 2. To simplify the discussion, assume the object $\mathcal{B}$ is grasped along planar facets perpendicular to the supporting plane. In this case the curvature dependent term in K_p is identically zero, and the grasp's stiffness matrix, specified in eq. (12), becomes:

$$K_p(q_0, 0) = -\sum_{i=1}^{k} \tilde{K}_i(q_0) + \begin{bmatrix} O_{2\times 2} & 0 \\ 0^T & \sum_{i=1}^{k} \boldsymbol{\rho}_i(\theta_0) \cdot f_i \end{bmatrix}. \tag{18}$$

In this formula $\tilde{K}_i(q_0)$ is the i^{th} contact stiffness matrix, $\boldsymbol{\rho}_i(\theta_0)$ is the vector from $\mathcal{B}$'s origin to the i^{th} contact point, and f_i is the i^{th} finger force at the equilibrium grasp. To synthesize a stable grasp or fixture arrangement, one must satisfy the three conditions $\alpha > 0$, $\beta > 0$, and $\gamma < \sqrt{\alpha}\beta$ specified by Theorem 2.Some guidelines how to achieve the three conditions are next discussed.

The $\alpha > 0$ condition: Since $\alpha = \lambda_{min}(M^{-1/2}(K_p)_s M^{-1/2})$, the condition $\alpha > 0$ is equivalent to the condition $\lambda_{min}\big((K_p)_s\big) > 0$. Based on (18), the symmetric part of K_p is given by

$$(K_p(q_0, 0))_s = -\sum_{i=1}^{k} \big(\tilde{K}_i(q_0)\big)_s + \begin{bmatrix} O_{2\times 2} & 0 \\ 0^T & \sum_{i=1}^{k} \boldsymbol{\rho}_i(\theta_0) \cdot f_i \end{bmatrix}.$$

The simple structure of $(K_p)_s$ leads to the following test for $\alpha > 0$.

Lemma 5.1 ($\boldsymbol{\alpha > 0}$ test). *Let $\mathcal{B}$ be held in a compliant k-finger equilibrium grasp with contact stiffness matrices $\tilde{K}_i(q_0)$ for $i = 1 \ldots k$. Write the symmetric 3×3 matrix $-\sum_{i=1}^{k} \big(\tilde{K}_i(q_0)\big)_s$ as*

$$-\sum_{i=1}^{k} \big(\tilde{K}_i(q_0)\big)_s = \begin{bmatrix} P_{11} & P_{12} \\ P_{12}^T & P_{22} \end{bmatrix}.$$

Then $\lambda_{min}\big((K_p)_s\big) > 0$ and hence $\alpha > 0$ when $-\sum_{i=1}^{k} \big(\tilde{K}_i(q_0)\big)_s$ is positive definite, and the preload forces satisfy the inequality:

$$\sum_{i=1}^{k} \boldsymbol{\rho}_i(\theta_0) \cdot f_i < P_{22} - P_{12}^T P_{11}^{-1} P_{12}.$$

Proof: Let us first express the matrix $-\sum_{i=1}^{k}\left(\tilde{K}_i(q_0)\right)_s$ in terms of P_{11}, P_{12}, and P_{22}:

$$(K_p(q_0,0))_s = \begin{bmatrix} P_{11} & P_{12} \\ P_{12}^T & P_{22} \end{bmatrix} + \begin{bmatrix} O & 0 \\ 0^T & \sum_{i=1}^{k} f_i(q)\cdot\boldsymbol{\rho}_i(\theta_0) \end{bmatrix}.$$

Consider now the transformation of the first summand:[3]

$$\begin{bmatrix} I & -P_{11}^{-1}P_{12} \\ 0 & 1 \end{bmatrix}^T \begin{bmatrix} P_{11} & P_{12} \\ P_{12}^T & P_{22} \end{bmatrix} \begin{bmatrix} I & -P_{11}^{-1}P_{12} \\ 0 & 1 \end{bmatrix} = \begin{bmatrix} P_{11} & 0 \\ 0^T & P_{22} - P_{12}^T P_{11}^{-1} P_{12} \end{bmatrix}.$$

Since the second summand of $(K_p)_s$ is invariant under this transformation, $(K_p)_s$ is related by the transformation to the block-diagonal matrix:

$$(K_p(q_0,0))_s \sim \begin{bmatrix} P_{11} & 0 \\ 0^T & P_{22} - P_{12}^T P_{11}^{-1} P_{12} + \sum_{i=1}^{k} f_i\cdot\boldsymbol{\rho}_i(\theta_0) \end{bmatrix}. \tag{19}$$

When A and P are $n \times n$ matrices such that A is non-singular and P symmetric, the eigenvalues of $A^T P A$ have the same sign as the eigenvalues of P. Based on this fact, the condition $\lambda_{min}\big((K_p)_s\big) > 0$ is equivalent to positiveness definiteness of the block diagonal matrix in (19). Since $P_{11} = \sum_{i=1}^{k} K_i > 0$, the latter matrix is positive definite iff its lower-right term is strictly positive. □

The proof of the lemma appears in the appendix. The lemma is based on the fact that planar grasps possess a special point, called the *center of compliance,* such that when $\mathcal{B}$'s origin is selected at this point the grasp's stiffness matrix becomes diagonal [26]. The term $P_{22} - P_{12}^T P_{11}^{-1} P_{12}$ is the grasp's rotational stiffness about its center of compliance. It follows that the preload forces can destabilize the grasp when $\sum_{i=1}^{k} f_i^0 \cdot \boldsymbol{\rho}_i < 0$ (Example 1). As discussed in Section 3, the individual matrices $(\tilde{K}_i)_s$ are negative definite for linear loading profiles and reasonable friction coefficients. Hence the only potentially destabilizing term is the sum $\sum_{i=1}^{k} \boldsymbol{\rho}_i(\theta_0) \cdot f_i$, which corresponds to the effect of the preload forces. The preload forces should therefore be sufficiently small so that they would not harm the positive definiteness of $(\tilde{K}_i)_s$ and consequently the positive definiteness of $M^{-1/2}(K_p)_s M^{-1/2}$.

Next consider the condition $\beta = \lambda_{min}\left(M^{-1/2} K_d M^{-1/2}\right) > 0$.

And the third condition for stability is $\gamma = \|M^{-1/2}(K_p)_{as} M^{-1/2}\| < \sqrt{\alpha}\beta$. To satisfy the **third condition** we need $\gamma = \|M^{-1/2}(K_p)_{as} M^{-1/2}\| < \sqrt{\alpha}\beta$. Specifically we have

$$(K_p)_{as} = \sum_{i=1}^{m} J_i^T R_i^T (K_i)_{as} R_i J_i,$$

[3]The transformation is induced by a translation of $\mathcal{B}$'s reference frame to the grasp's center of compliance.

and recall that

$$K_i = \begin{bmatrix} \frac{4G\sqrt{R\delta_i^n}}{1-\nu} & 0 \\ \frac{8GR\delta_i^t}{3\sqrt{R\delta_i^n}(2-\nu)} & \frac{16G\sqrt{R\delta_i^n}}{3(2-\nu)} \end{bmatrix}.$$

Substituting Walton loading path $c_i = \frac{\delta_i^t}{\delta_i^n}$ yields

$$K_i = G\sqrt{R\delta_i^n} \begin{bmatrix} \frac{4}{1-\nu} & 0 \\ \frac{8c_i}{3(2-\nu)} & \frac{16}{3(2-\nu)} \end{bmatrix}.$$

Which its skew-symmetric part is

$$(K_i)_{as} = G\sqrt{R\delta_i^n} \begin{bmatrix} 0 & -\frac{8c_i}{3(2-\nu)} \\ \frac{8c_i}{3(2-\nu)} & 0 \end{bmatrix}.$$

Note that the maximum eigenvalue of $(K_i)_{as}$ depends on the value of $|c_i|$. Small $|c_i|$ correspond to penetrations which are more in the normal direction and consequently forces that are more normal than tangential. Moreover, small $|c_i|$ introduces small asymmetric part of K_i and help satisfy the third condition of the theorem. Thus the third condition introduce an upper bound to the sum of the $|c_i|$s. However this is not the only condition on the $|c_i|$s. From proposition 3.2 we have the following condition for $(K_i)_s$ to be positive definite:

$$|c_i| < \sqrt{\frac{12(2-\nu)}{(1-\nu)}}.$$

We also have an upper bound on $|c_i|$ which guarantees that the contact force is within its friction cone as follows:

$$c_i^f = \frac{F_i^t}{F_i^n} = c_i \frac{2(1-\nu)}{(2-\nu)} < \mu$$

Finally, the third upper bound on $|c_i|$ is from the third condition of Corollary **??**

$$\|M^{-1/2}(K_p)_{as}M^{-1/2}\| < \sqrt{\alpha}\beta$$

as discussed before. The selection of $|c_i|$s value is such that it satisfies all these three upper bounds. This together with the other two conditions, are sufficient for the equilibrium of the grasping arrangement to be *locally asymptotically stable*. □